

# OPTIMIZATION OF THE MECHANICAL STRUCTURE OF INDUSTRIAL ROBOTS USED IN WELDING OPERATIONS, USING THE FINITE ELEMENT METHOD

Răzvan POPA<sup>\*</sup>, Dorel ANANIA<sup>\*\*</sup>, Adrian GHIONEA<sup>\*\*</sup>

<sup>\*</sup>IFM Electronic S.R.L., Romania

<sup>\*\*</sup>Politehnica University of Bucharest, Romania

**Abstract:** This paper is about choosing the optimum variant, from the constructive-geometrical and material points of view, for a structure element within the construction of an industrial robot. We have used finite elements analysis (FEA) for optimizing the robot's forearm as regards the stress it is subject to, without influencing the technical-functional parameters. The articulated arm-type industrial robot studied below is dedicated to welding applications, being integrated in a robotized flexible cell for electric arc welding, choosing the optimum variant of the robot's forearm.

**Key words:** industrial robot, optimization, finite element analysis, welding cell

## 1. Introduction

The development of the world's industry in the latest decades and the increase in the manufacturing of equipment and apparatus have led to the acceleration of the utilization of robots in the welding processes, this becoming the widest domain of using articulated arm-type industrial robots. Also, the upgrading of the machine parts, mechanical transmissions, drive engines, sensorial and control systems has made it possible to create industrial robots with dynamic performance and high precision, which has extended the welding robotic applications [1]. These technical and functional performances of the industrial robots are imposed by the welding process specific parameters [2].

The arc welding robots must provide a continuous movement and a precise positioning of the welding head at the joining line (welding joint). One of the requirements of the robotic electric arc welding consists in the precise positioning of the welding head ( $\pm 0.5 \dots 1$  mm) and it depends on the following factors:

- the stability of the mobile mechanical elements of the robot when making various movements and its coming back at the end of the operation;
- the possible gaps of fastening the welding head on the flange of the last axis of the robot;
- the possible deformations of the welding head and bending of the electrode wire tip;
- a proper speed for making various movements which should be continuously adjustable ( $0 \div 2.5$  m/s) and at least one of the movements should be very rapid, the one of the rotating arm ( $1 \div 1.5$  m/s) [2].

## 2. Case study

### 2.1. Application description

The industrial robot analyzed below in view to optimizing the tubular forearm is articulated, having 6-axis and being integrated in a robotic welding flexible cell for small and middle parts.

The main components of welding cell are: industrial robots, robot's positioned, positioners for the welded parts, robot's controller, welding torch, welding equipments, wire drive unit, cleaning unit for the welding torch, safety guarding, safety optical barrier (figure 1).

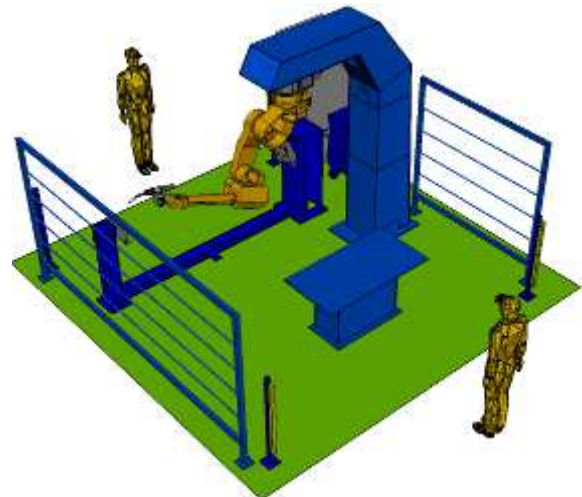


Figure 1. Layout welding flexible cell

The tubular forearm (figure 2, element 4) is contained in the carcass, being at the same time a tubular shaft, in order to make the first movement of

the Roll-type orientation system (4th degree of freedom/axis 4).

For this study, we have calculated the reduced loadings at the main axes X, Y, Z of the mass centers for: end-effector, orientation system and the element studied (figure 2, tubular forearm - element 4).

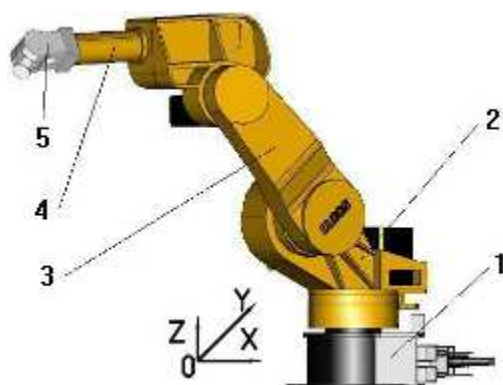


Figure 2. Industrial robot: 1 - robot base; 2 - wrist; 3 - arm; 4 - forearm; 5 - orientation system

The stress calculation was made depending on:

- the materials used for the component parts;
- the constructive dimensions of the elements necessary for the existent cinematic chains of the forearm;
- the constructive and cinematic parameters of the robot (maximum strokes, angular speeds, distances between the rotation axes) [3].

Calculations were made for:

- masses and mass centres for: end-effector, orientation system, tubular forearm, forearm carcass;
- reduced forces in each mass centre due to the movement of the rotation torques, static loadings; reduced loadings at the main axes of the mass centres for end-effector, orientation system and tubular forearm;
- reduced loadings on the studied element: in its mass centre (due to its own mass); reduced loadings of the end-effector's mass and of the orientation system on the fastening flange of the tubular forearm.
- reduced loadings on the studied element for five variations of the forces, in view of obtaining a simulation of the elastic come-back variation in dynamic regime of the studied element.

**Remark:** Calculations of the masses, reduced forces and reduced loadings were made by means of a specific computer program.

The results obtained subsequent to the analysis:

- the variation diagrams of the elastic come-backs of the tubular forearm for deformations obtained at

the following stresses: Main Stress Maxx; Main Stress Middle; Main Stress Min; Force on axis X; Force on axis Y; Force on axis Z; Pressure on plan XY; Pressure on plan YZ; Pressure on plan ZX; Deformation after axis X; Deformation after axis Y; Deformation after axis Z and Resultant deformation.

- solutions for structure optimization and results comparison.

## 2.2. Description of the robot

**Kineamtics:** the kinematics parameters are on the Closs leaflet.

**Construction:** the studied robot is in anthropomorphic construction, made of an aluminum-magnesium alloy cast under pressure.

Its functional characteristics are:

- number of axes: 6;
- maximum manipulated mass: 10 kg;
- drive: electronically adjusted alternating current servomotor mounted on each axis;
- position measurement: digital, absolute (resolver);
- positioning error:  $\pm 0.1$  mm;
- work space: spherical, with the radius of about 4100 mm;
- dimensions: supporting surfaces:  $460 \times 730$  mm;
- mass: 245 kg;
- possibility of axes rotation: Axis 1:  $340^\circ$ ; Axis 2:  $225^\circ$ ; Axis 3:  $292^\circ$ ; Axis 4:  $360^\circ$ ; Axis 5:  $270^\circ$ ; Axis 6:  $600^\circ$ ;
- maximum axes speed: Axis 1:  $148^\circ/\text{s}$ ; Axis 2:  $130^\circ/\text{s}$ ; Axis 3:  $165^\circ/\text{s}$ ; Axis 4:  $300^\circ/\text{s}$ ; Axis 5:  $300^\circ/\text{s}$ ; Axis 6:  $400^\circ/\text{s}$ ;
- the materials used to make the component parts: the non-standardized component parts, such as shafts, bushes, etc., are made of OLC 45 steel, having the following features: density:  $7800 \text{ kg/dm}^3$ ; elasticity module:  $E = 210000 \text{ N/mm}^2$ ; Poison coefficient: 0.3. The carcass and tubular shaft are made of aluminum (Al) alloy, having the following features: density  $2700 \text{ kg/dm}^3$ ; elasticity module  $E = 71015.9 \text{ N/mm}^2$ ; Poison coefficient: 0.33.

## 3. Determination of loadings on the robots' forearm

### 3.1. Determination of masses and mass centres for: end-effector, orientation system, tubular forearm, forearm carcass

The masses of the main sub-assemblies were calculated by means of a specific computer program. In this program, the following equations were implemented [4]:

$$\begin{aligned} X_G &= \frac{\sum X_{Gi} \cdot m_i}{\sum m_i}; \\ Y_G &= \frac{\sum Y_{Gi} \cdot m_i}{\sum m_i}; \\ Z_G &= \frac{\sum Z_{Gi} \cdot m_i}{\sum m_i}, \end{aligned} \quad (1)$$

where:  $X_G, Y_G, Z_G$  – coordinates of the mass centres.

For the orientation sub-system, the elements strictly belonging to it were taken into account (without the drive tubular shafts).

For the calculated element, its own mass and the tubular drive shafts crossing through it were taken into account. For the forearm carcass, all the elements within it were taken into account (engines, harmonic reducers, drive shafts, rotary gears, etc).

### 3.2. Determination of the reduced forces in each mass centre; static loadings and reduced loadings at the main axes of the mass centres

The reduced forces in the mass centers for the end-effector, orientation system and the tubular forearm, are calculated by means of a specific computer program, where we implemented the calculation equations for centrifugal and tangential forces obtained due to the successive movement of each torque (the other torques being considered rigid).

The forces obtained on each mass centre of interest were reduced at the main axes of the respective mass centre [5].

In order to make the calculation, the positions of the mass centres of interest were established depending on the 3rd rotation axis, this one being the forearms' rotation axis.

The acceleration time from zero  $m/sec^2$  to the maximum speed on each axis is of 0.5 sec.

Within the calculation program on the computer, the following equations were implemented:

$$\begin{aligned} F_{cf} &= m \cdot \omega^2 \cdot R; \\ F_{tg} &= m \cdot \varepsilon \cdot R; \\ \varepsilon &= \frac{\Delta\omega}{\Delta t}; \\ G &= m \cdot g, \end{aligned} \quad (2)$$

where:  $F_{cf}$  – centrifugal force, in N;

$F_{tg}$  – tangential force, in N;

$\omega$  – angular velocity, in rad/sec;

$R$  – gyration radius, in mm;

$G$  – weight in mass centre, in N;

$m$  – element mass, in kg;

$g$  – gravitational acceleration, in  $m/sec^2$ .

### 3.3. Determination of the reduced loadings on the studied element: in its mass centre; reduced loadings of the end-effector's mass and of the orientation system

The loadings due to the mass centres of the orientation sub-system and end-effector will reduce at the fastening flange with the forearm in two points, according to the fundamental scheme from figure 3:

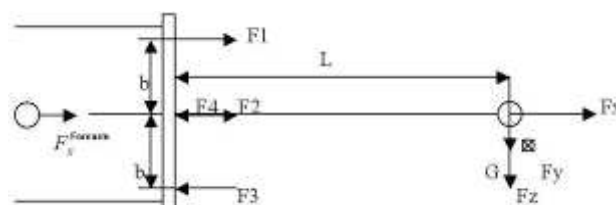


Figure 3. Scheme of the loadings on the fastening flange of the industrial robot's forearm

The equations used for calculating the reduced forces at the level of the studied element, specifically of the industrial robot's forearm [6], are the following:

$$F_1 = \frac{F_{xrez}}{4} + \frac{(F_{yrez} + G) \cdot L}{2b} + \frac{F_x^{forearm}}{4}; \quad (3)$$

$$F_2 = \frac{F_{xrez}}{4} + \frac{F_y \cdot L}{2b} + \frac{F_x^{forearm}}{4}; \quad (4)$$

$$F_3 = \frac{F_{xrez}}{4} - \frac{(F_{yrez} + G) \cdot L}{2b} + \frac{F_x^{forearm}}{4}; \quad (5)$$

$$F_4 = \frac{F_{xrez}}{4} + \frac{F_y \cdot L}{2b} + \frac{F_x^{forearm}}{4}, \quad (6)$$

where:  $F_{1,2,3,4}$  – reduced forces, in N ( $F_1 = 1792$  N;  $F_2 = 774.61$  N;  $F_3 = 1163.61$  N;  $F_4 = 146.19$  N);  $F_{x,y,zrez}$  – resultant forces, in N;  $L$  – element length, in mm.

The determined loadings were applied on the 3D model analyzed using the finite element methods (figure 4).

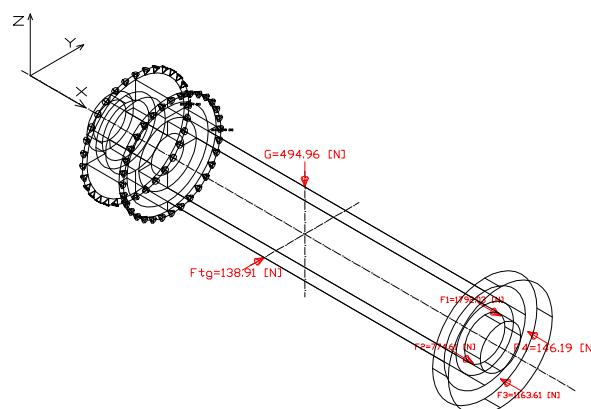


Figure 4. Scheme of the loadings on the robot's forearm

#### 4. Results regarding the elastic come-backs of the robot's tubular forearm obtained trough FEA

The purpose of using the finite element method (FEA) and of choosing the elements within the structure of the industrial robots is to optimize the mechanical system of the robots making the movement and welding operation [7].

The finite element method is one of the strongest numerical calculation method used in engineering [8]. Basically, the basic idea of this method is to approximate the unknown field function (temperature, deformation, flowing speed, and pressure) with a *spline* function, so that, on sufficiently small sub-domains, called finite elements, the approximation should be sufficiently close to the precise solution. This approximation is introduced in the condition of extreme (minimum) of the functional associated to the system of differential equations governing the phenomenon [9]. We obtain, therefore, a linear algebraic system or an ordinary differential equations system, according to the treated problem, which is in static or dynamic regime.

The following figures present the diagrams resulted subsequent to the analysis made by the computer program, of the elastic come-backs of the robot's forearm studied [10, 11, 12].

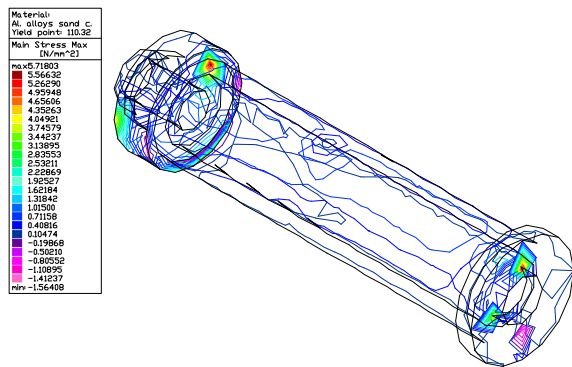


Figure 5. Main stress maximum

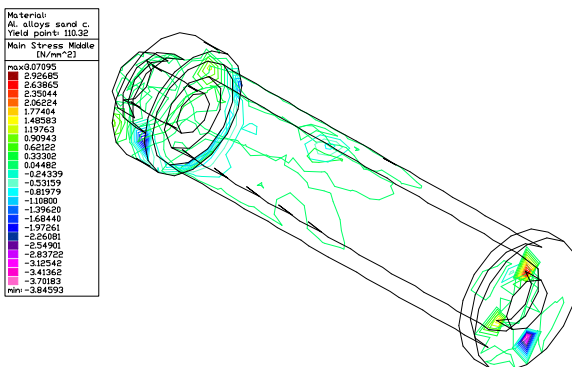


Figure 6. Main stress middle

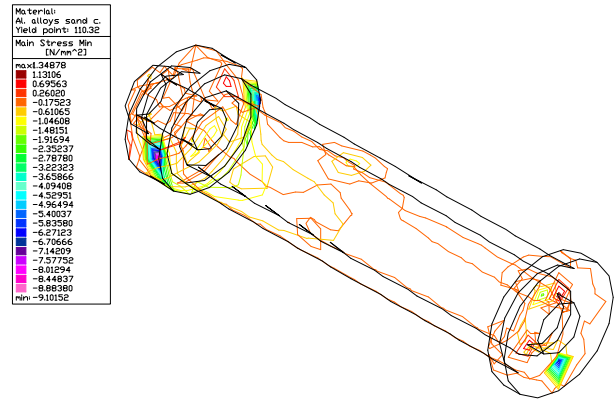


Figure 7. Main stress minimum

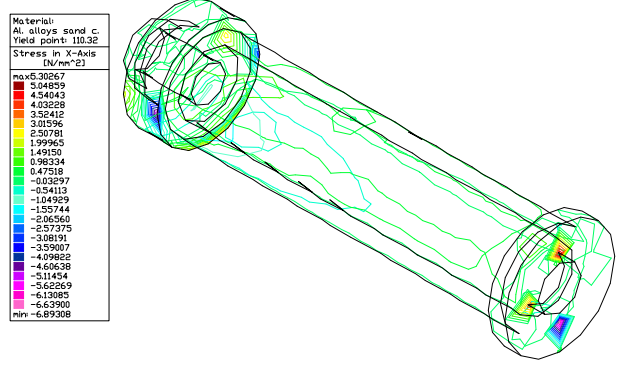


Figure 8. Stress in X-axis

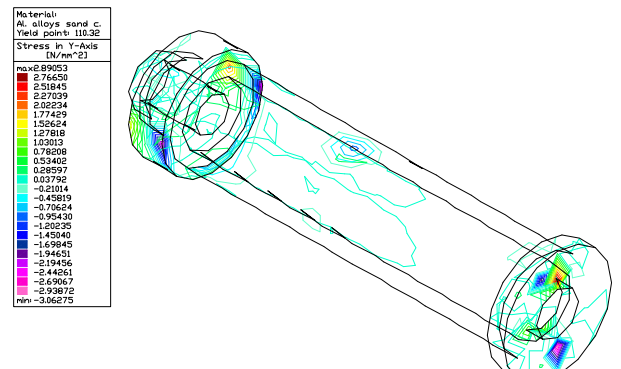


Figure 9. Stress in Y-axis

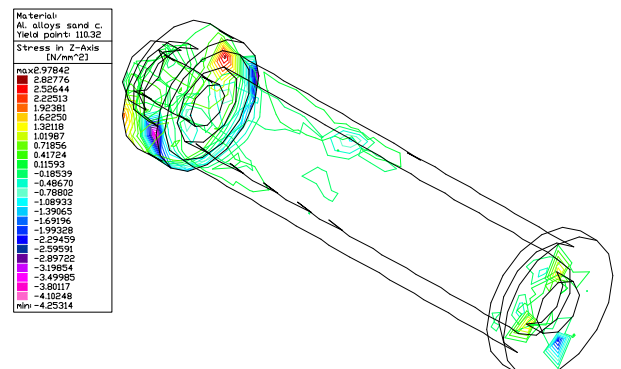


Figure 10. Stress in Z-axis

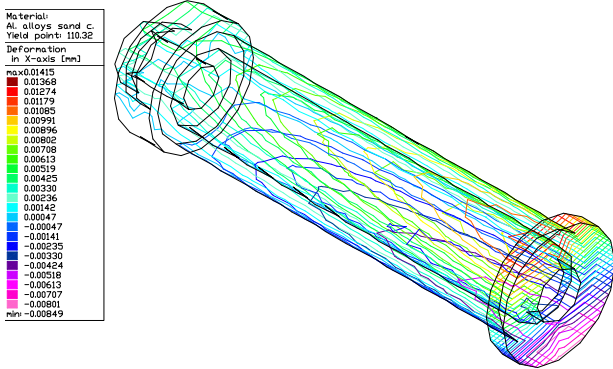


Figure 11. Deformation in X-axis

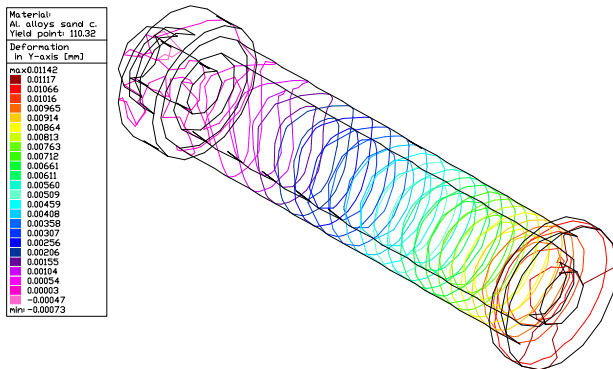


Figure 12. Deformation in Y-axis

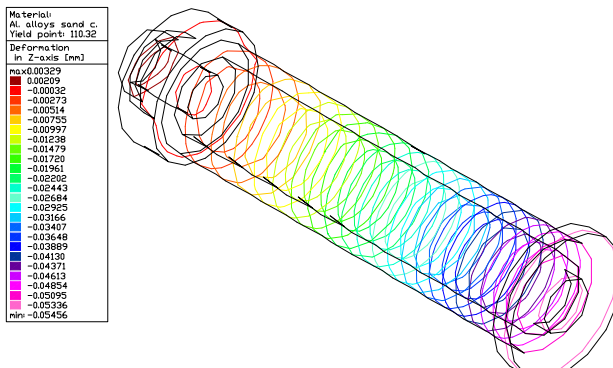


Figure 12. Deformation in Z-axis

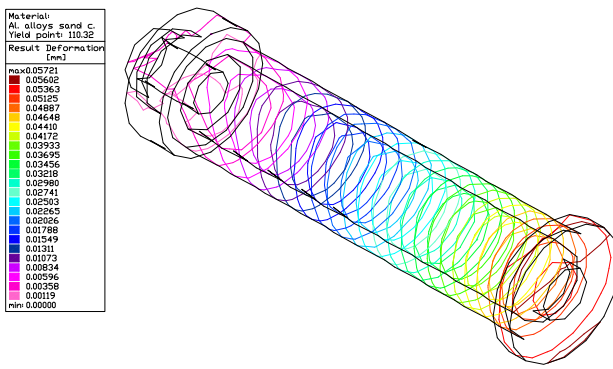


Figure 13. Result deformation

## 5. Experimental results

A comparative analysis was made for the following aspects regarding the robot's forearm:

- deformation on the axes X, Y and Z;
- stress on the axes X, Y and Z;
- main stress maximum, for the forearm made with an increased the forearm's thickness, 5 mm higher than the solution proposed to make the forearm from steel.

Figure 14 presents the deformation on axis x for a robot's forearm with increased thickness, of 5 mm, of the outside wall, as compared to the analyzed variant.

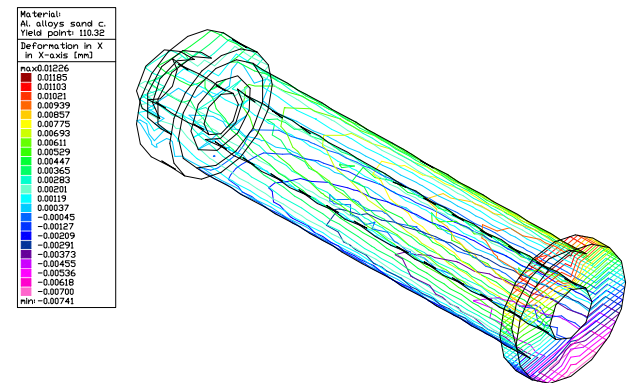


Figure 14. Deformation in X-axis for the forearm with 5 mm higher thickness

Figure 15 presents the deformation on axis x for a robot's forearm made of S235JR (equivalent with OL37 STAS 500/2-80) quality laminated steel.

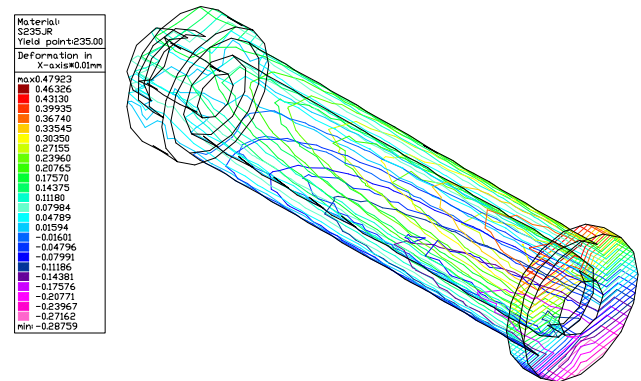


Figure 15. Deformation in X-axis for the forearm made from steel S235JR

For forearm with higher thickness of the wall, the maximum deformation is of 0.01226 mm and the minimum deformation is of 0.00741 mm, and as regards the steel forearm, the maximum deformation is of 0.0047923 mm and the minimum deformation is of 0.0028759 mm.

In conclusion, as compared to the analyzed solution, which made the object of the case study, where the maximum deformation was of 0.1415 mm and the minimum one was of 0.00849 mm, it resulted that, in case of the forearm with higher thickness of the wall, the deformations are smaller, and, in case of the quality laminated steel forearm, the deformations are even smaller, but the main disadvantage of these solutions is the mass increase.

Figure 16 and 17 present the value for the deformations on the Y and Z axes.

In both cases, can be seen a much smaller deformation than in the case of the proposed solution, but, the same, the main disadvantage consists in the mass increase, which, in case of industrial robots, is a very important factor.

The maximum values of the deformations on the Y and Z axes are the highest in case of the analyzed solution (deformations on axis Z: max: 0.00329 mm and min: -0.054 mm; deformations on axis Y: max: 0.01142 mm and min: -0.00073 mm) as compared to the deformations obtained in case of the forearm with higher thickness of the wall (deformations on axis Z: max: 0.00308 mm and min: -0.04767 mm; deformations on axis Y: max: 0.00959 mm and min: -0.0006632 mm).

Thus, tubular forearm produced by Closs, made of aluminium, compared to other variance analysis has deformations on the three axis X, Y and Z the highest, but the smallest mass.

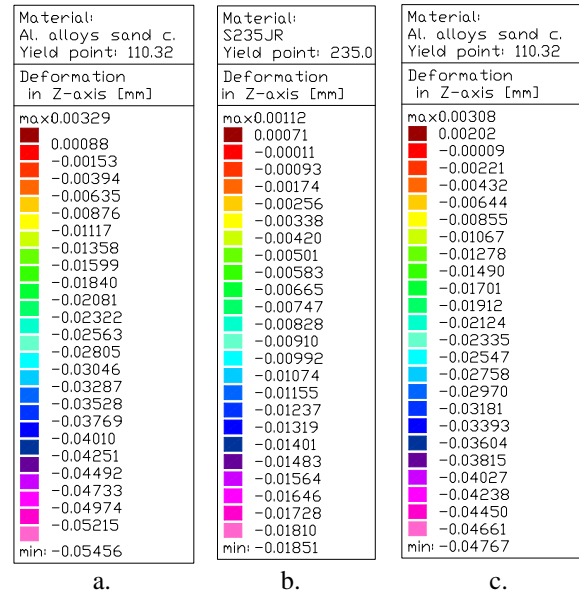


Figure 17. Deformation in Z-axis for the forearm: a - analyzed model; b. made from steel; c. with 5 mm higher thickness

The smallest deformations are obtained in case of the steel forearm (deformations on axis Z: max: 0.00112 mm and min: -0.01851 mm; deformations on axis Y: max: 0.00386 mm and min: -0.000246 mm). In terms of deformation, it can be concluded that this option is optimal, but at the same time has the highest mass.

The tables below present the stresses on the three axes X, Y and Z, for the three variants of robot's forearm: the analyzed model, made from steel and with higher thickness of the outside wall.

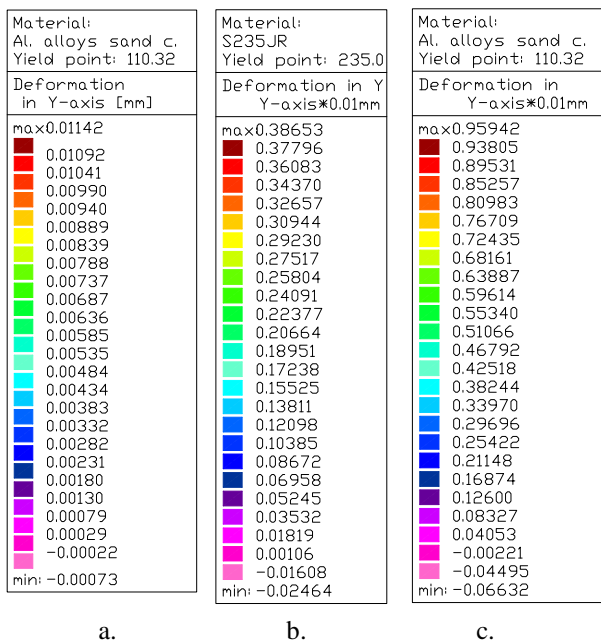


Figure 16. Deformation in Y-axis for the forearm: a - analyzed model; b. made from steel; c. with 5 mm higher thickness

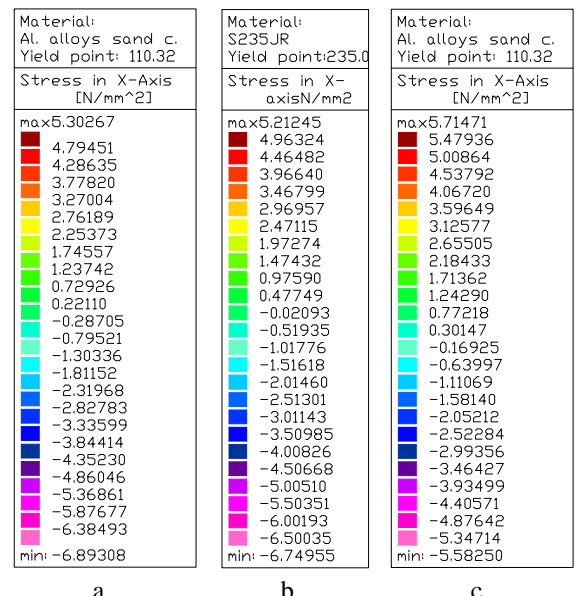


Figure 18. Stress in X-axis for the forearm: a. analyzed model; b. made from steel; c. with 5 mm higher thickness

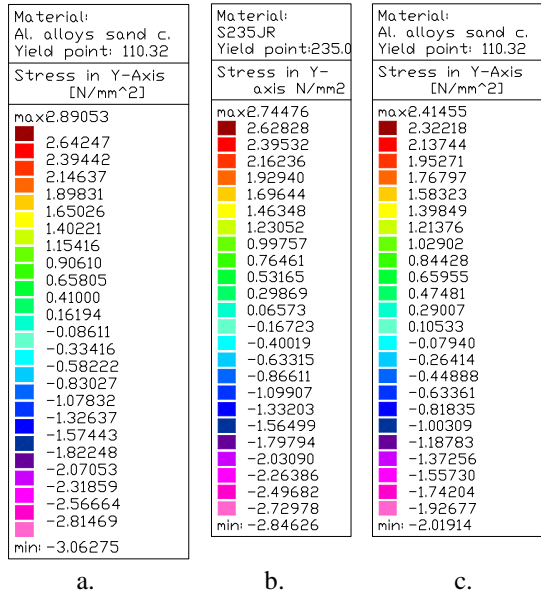


Figure 19. Stress in Y-axis for the forearm: a. analyzed model; b. made from steel; c. with 5 mm higher thickness

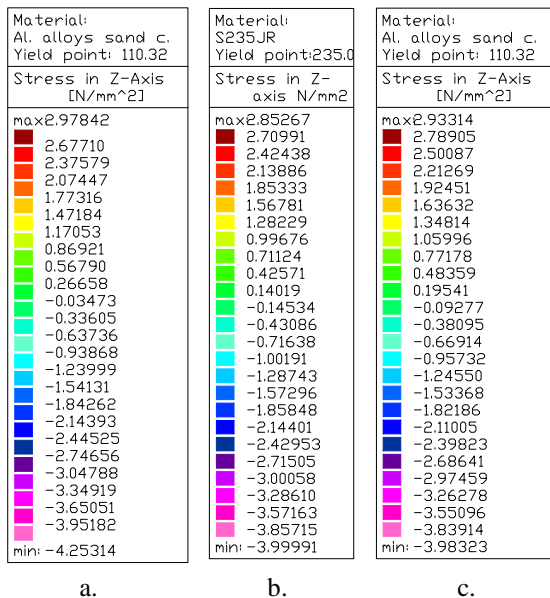


Figure 20. Stress in Z-axis for the forearm: a. analyzed model; b. made from steel; c. with 5 mm higher thickness

From the point of view of the stresses on the main axes, we see that, on axis X, the lowest stress maximum is for the steel forearm (5.212 N/mm<sup>2</sup>), as compared to the analyzed solution (5.306 N/mm<sup>2</sup>).

It should be noticed the fact that the maximum stress of the forearm with higher thickness (5.71 N/mm<sup>2</sup>) is higher than the one of the analyzed solution.

From the point of view of the minimum stress, the forearm with higher thickness, this is the closest to zero (- 5.58 N/mm<sup>2</sup>), being followed by the steel forearm (- 6.749 N/mm<sup>2</sup>) and the analyzed solution (-6.893 N/mm<sup>2</sup>).

On axis Y, the highest stress maximum appears in case of the analyzed solution (2.8905 N/mm<sup>2</sup>), being followed by the steel forearm (2.74476 N/mm<sup>2</sup>) and by the forearm with higher thickness (2.41455 N/mm<sup>2</sup>). In case of the minimum stresses, things are the same: analyzed solution (- 3.0627 N/mm<sup>2</sup>), steel forearm (- 2.84626 N/mm<sup>2</sup>) and thickened forearm (-2.01914 N/mm<sup>2</sup>).

On axis Z, the highest stress maximum appears in case of the analyzed solution (2.978 N/mm<sup>2</sup>), being followed by the one of the thickened forearm (2.93314 N/mm<sup>2</sup>) and the steel forearm (2.853 N/mm<sup>2</sup>). In case of the minimum stresses, the following order appears: analyzed solution (- 4.2531 N/mm<sup>2</sup>), steel forearm (- 3.9991 N/mm<sup>2</sup>), thickened forearm (- 3.98323 N/mm<sup>2</sup>).

Figure 21 presents the maximum stresses for the three variants of the robot's forearm.

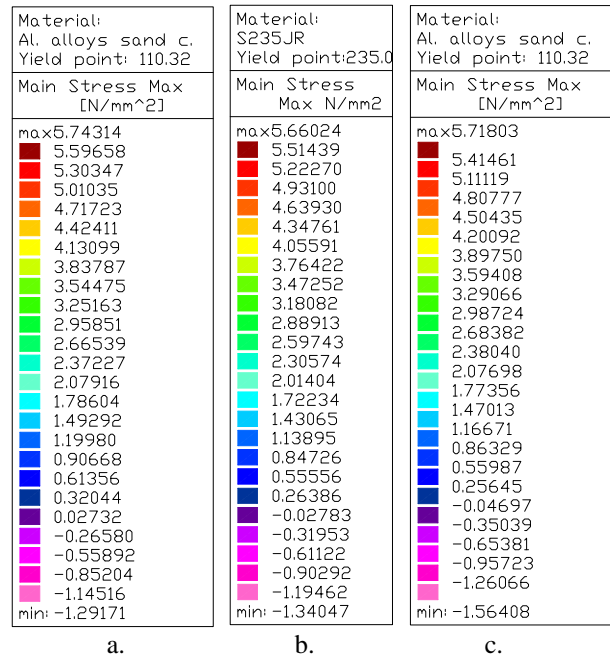


Figure 21. Main Stress Maximum for the forearm: a. analyzed model; b. made from steel; c. with 5 mm higher thickness

From the point of view of main stress maximum, we see that, for the analyzed solution, the maximum stress is the highest (5.74314 N/mm<sup>2</sup>), being followed by the value for the thickened forearm (5.71803 N/mm<sup>2</sup>) and the one for the steel forearm (5.66024 N/mm<sup>2</sup>).

The minimum value of the maximum stress is the one as in case of the analyzed solution (-1.2917 N/mm<sup>2</sup>), being followed by the one of the steel forearm (-1.34047 N/mm<sup>2</sup>), and the one of the

forearm with increased thickness ( $-1.56408 \text{ N/mm}^2$ ).

Following the analysis of stress for the three variants of tubular forearms, noticed that they are influenced differently on the three axes X, Y and Z.

## 6. Conclusions

The described analyses shows an example of using FEA in order to find the optimum variant for a structure element of an welding industrial robot. Also, the quality and the cost can be optimized to achieve a robust structure for the robot.

Considering the analysis made above, on the three variants of tubular forearm, we draw the conclusion that, from the point of view of deformations and stresses on the three axes X, Y and Z, the optimum solution is to make the tubular forearm from steel.

From the point of view of the forearms' own mass, it can be remarked that: for the steel forearm, we have 58.1611 kg, for the forearm with increased thickness, we have 27.1636 kg, and for the analyzed solution, we have 20.1041 kg.

As the difference between the deformations and stresses the forearm is subject to, obtained for the three proposed solutions, is very small, and the mass differences are significant, we choose the first analyzed solution (forearm produced by Closs).

In order to make the forearm rigid, the following solutions may be adopted:

- tubular element provided with reinforcement ribs, either inside, or outside, next to the sections where the stress is maximum;
- making the forearm from other material (for example, laminated steel) the main disadvantage of this method is that the forearm's mass increases;
- changing the forearm's shape, for example, a taper shape, the big base next to the higher stress;
- the construction of the forearm with a higher thickness of the wall and of the fastening flange.

## References

1. Joni, N., Trif, N. (2005) *Sudarea robotizată cu arc electric (Robotized electric arc welding)*. Lux Libris Publishing House, ISBN 973-9458-34-3, Braşov, Romania (in Romanian)
2. Joni, N., Trif, N. (2007) *Aplicații industriale ale sudării robotizate cu arc electric (Industrial applications of robotized arc welding)*. Proceeding of International Conference ASR Sudura, 26-28 September, Sudura Publishing House, Timișoara, Romania (in Romanian)
3. \*\*\* *Industrial Robots Catalogues 2010*. Available from: www.cloos.de, Accessed: 27/11/2010
4. Nicolescu, A., (1997) *Proiectarea roboților industriali. Partea I – Concepte fundamentale. Criterii de analiză și sinteză optimală utilizate în proiectarea R.I., Construcția de mașini (Industrial Robot Design 1st Part – Fundamental Concepts. Analysis and Synthesis Criteria used in Industrial Robot Design, Tool Construction)*. No. 4-5, p. 11-20, Bucharest, Romania (in Romanian)
5. Nicolescu, A. (1997) *Proiectarea roboților industriali. Partea I – Conceptul sistemic unitar de robot integrat în mediul tehnologic. Subsystemul mecanic al R.I. Motoare de acționare utilizate la R.I. (Industrial Robot Design 1st Part – Unit Systemic Concept of Robot Integrated in the Technological Environment. Mechanical Sub-system of the I.R. Drive engines used at R.I.)*. Politehnica University of Bucharest, Romania (in Romanian)
6. Dorin, Al., Dobrescu, T., Pascu E.N., Ivan I. (2011) *Cinematica roboților industriali (Kinematics of Industrial Robots)*. BREN Publishing House, ISBN 978-973-648-970-8, Bucharest, Romania (in Romanian)
7. Zapciu, M., Anania, D., Bisu, C. (2005) *Concepție și fabricație integrate (Integrated design and manufacturing)*. Bren Publishing House, ISBN 973-648-481-5 Bucharest, Romania (in Romanian)
8. Anania, D., Mohora, C. (2008) *Research Concerning FEA for a Machine Structure Assembly*. Proceedings of the 1st WSEAS International Conference on Visualization, Imaging and Simulation (VIS'08), Mathematics and Computers in Science and Engineering, ISSN 1790-2769, ISBN: 978-960-474-022-2
9. Liu, G.R., Quek, S. S. (2003) *The Finite Element Method: A Practical Course*. An imprint of Elsevier Science, 2003, ISBN 0-7506-5866-5
10. Ispas, C., Zapciu, M., Mohora, C., Anania, D., (2006) *Product development using CAD-CAM-CAE software and internet facilities*. The International Conference of the Carpathian Euro-Region Specialists in Industrial Systems, Baia Mare, Romania, ISSN 1224-3264
11. Zapciu, M., Anania, D., Tilina, D. (2006) *Data exchange compatibility between cad/cam software in integrated design process fo the technical product*. The International Conference of the Carpathian Euro-Region Specialists in Industrial Systems, Baia Mare, Romania, ISSN 1224-3264
12. Ispas, C., Zapciu, M., Anania, F.D. (2009) *Diagnose of industrial robots accuracy performance using qc10 ballbar system*. Proceedings Optimization of the robots and manipulators, 28-31 May 2009, p. 81-85, ISSN 2066-3854, Bren Publishing House, Bucharest, Romania